HHS Public Access

Author manuscript

Nat Neurosci. Author manuscript; available in PMC 2019 March 06.

Published in final edited form as:

Nat Neurosci. 2016 October ; 19(10): 1341–1347. doi:10.1038/nn.4372.

Hypothalamic arcuate nucleus tyrosine hydroxylase neurons play orexigenic role in energy homeostasis

Xiaobing Zhang and **Anthony N van den Pol**

Department of Neurosurgery, Yale University School of Medicine, New Haven, Connecticut, USA.

Abstract

Energy homeostasis, food intake, and body weight are regulated by specific brain circuits. Here we introduce an unexpected neuron, the tyrosine hydroxylase (TH) neuron of the arcuate nucleus (ARC), that we show makes an orexigenic contribution. Optogenetic stimulation of mouse ARC TH neurons increased food intake; attenuating transmitter release reduced body weight. Optogenetic stimulation of ARC TH cells inhibited pro-opiomelanocortin (POMC) neurons through synaptic mechanisms. ARC TH cells project to the hypothalamic paraventricular nucleus; optogenetic stimulation of ARC TH axons inhibited paraventricular nucleus neurons by dopamine and GABA co-release. Dopamine excited orexigenic neurons that synthesize agouti-related peptide and neuropeptide Y but inhibited anorexigenic neurons that synthesize POMC, as determined by whole cell recording. Food deprivation increased c-fos expression and spike frequency in ARC TH neurons. The gut peptide ghrelin evoked direct excitatory effects, suggesting these neurons monitor metabolic cues. Together these data support the view that ARC TH cells play an unrecognized and influential positive role in energy homeostasis.

Obesity together with its associated health problems is reaching epidemic proportions in many countries, underlining the critical need for understanding how the brain regulates food intake[1,2]. Several brain systems, including the hypothalamus, midbrain, and brainstem, contribute to physiological energy homeostasis[3,4], and several neuron types are involved. Neurons that synthesize pro-opiomelanocortin (POMC neurons) or agouti-related peptide and neuropeptide Y (NPY/AgRP neurons) in the hypothalamic ARC are important to energy homeostasis[5–11]. Here we ask whether a third type of cell in the ARC that synthesizes TH may also contribute to neural control of energy balance.

Previous reports related to the role of TH neurons in food intake focused on cells from the midbrain ventral tegmental area or substantia nigra that synthesize dopamine[12–14]. A common theme has been that TH neurons that release dopamine may influence food intake by dopaminergic modulation of the hedonic properties of food and food intake[13,14]. Here we

Correspondence should be addressed to A.N.v.d.P. (anthony.vandenpol@yale.edu).

AUTHOR CONTRIBUTIONS

X.Z. and A.N.v.d.P. designed the experiments. X.Z. performed experiments and analyzed the data. X.Z. and A.N.v.d.P. cowrote the manuscript.

COMPETING FINANCIAL INTERESTS

The authors declare no competing financial interests.

Note: Any Supplementary Information and Source Data files are available in the online version of the paper.

introduce another population of TH cells from the ARC that is sensitive to hunger state and long-distance hunger signals, and directly modulates the activity of hypothalamic neurons involved in energy homeostasis by release of the neuromodulator dopamine or the fast amino acid inhibitory transmitter GABA in the ARC and hypothalamic paraventricular nucleus.

RESULTS

Identification of arcuate TH neurons

To selectively generate gene expression only in TH neurons from one among multiple TH-producing loci, we combined a Cre-dependent viral vector with glass pipette microinjection into the ARC in transgenic mice in which Cre recombinase expression was driven by the gene promoter for TH, the rate-limiting enzyme in dopamine synthesis. That the cells we study here express TH was corroborated with TH immunofluorescence (Supplementary Fig. 1)[15]. This approach allowed us to selectively stimulate ARC TH neurons, a strategy that would not be possible by transgenic mouse crossbreeding alone, and also avoids complications arising from potential transient expression of Cre recombinase under control of the TH promoter in some cells during early development[16].

To determine whether ARC TH neurons might coexpress POMC or NPY/AgRP, we used combinations of immunostaining, transgenic mice, and AAV vectors. Our data indicate that TH neurons constitute a unique population of arcuate neurons different from the POMC and NPY/AgRP cells; neither POMC nor NPY/AgRP neurons expressed detectable TH (Fig. 1 and Supplementary Figs. 2 and 3); similarly, TH neurons showed no expression of NPY/AgRP or POMC.

Optogenetic activation of TH neurons increases feeding; silencing reduces body weight

ARC TH cells have received little if any attention relating to a potential role in energy homeostasis. We used optogenetics to determine the behavioral effect of stimulating ARC TH neurons using Cre-dependent ChIEF[17]. Optogenetic stimulation of ChIEF-expressing TH cells in ARC brain slices generated a robust increase in spike frequency of both bursting and nonbursting neurons (Supplementary Figs. 4 and 5). Photostimulation of ARC TH neurons in mice evoked an increase in food intake (Fig. 2a–g) as determined by measuring the amount of food consumed during the period of stimulation; photostimulation of control mice that did not express ChIEF evoked no change in food intake (Fig. 2a–g).

To silence the ARC TH neurons, a Cre-dependent AAV that expressed the tetanus toxin analog TeNT[18] was microinjected into the ARC of mice crossbred to a Swiss Webster background, resulting in mice bigger than many inbred strains. TeNT-GFP was selectively expressed in ARC TH neurons (Fig. 2h and Supplementary Fig. 6). These mice were followed for over 5 months. Whereas control mice showed a normal weight gain over this period, the weight gain of TeNT-expressing mice was substantially reduced (Fig. 2h–j). These data show that the influence of ARC TH neurons is not transient, and that when ARC TH neuron signaling is attenuated, a long term reduction in body weight set point occurs, with 27% less body weight gain 3 months after gene vector administration.

Optogenetic activation of TH cells inhibits POMC neurons

We microinjected Cre-dependent AAV-CAG-DIO-tdTomato-ChIEF into the dorsomedial ARC, where the highest concentration of dopamine in TH neurons is found[19]; mice expressed Cre driven by the TH promoter and revealed a high density of TH axons and boutons terminating not only in the median eminence, but also on nearby cells within the ARC (Fig. 3a–d). We also identified red fluorescent ARC efferent axons in the hypothalamic ventromedial nucleus and dorsomedial nucleus. To identify potential postsynaptic partner neurons, we crossed TH-Cre mice with POMC-GFP and NPY-GFP reporter mice. To study transmitter responses related to TH efferent axons, we again used optogenetics with a Cre-dependent ChIEF-AAV injected into the ARC.

Photostimulation of ARC ChIEF-expressing cells (Supplementary Figs. 4 and 5) evoked a substantial increase in the amplitude and frequency of inhibitory postsynaptic currents (IPSCs) in 17 of 22 POMC neurons (Fig. 3h–j and Supplementary Fig. 7a), which was phase locked with 1 Hz photostimulation. Evoked IPSCs were largely blocked by the $GABA_A$ receptor antagonist bicuculline (30 μM, Fig. 3g), consistent with a previous immunocytochemical report suggesting coexpression of GABA in ARC TH neurons[20]. Both photostimulation (20 Hz) of ARC TH neurons and dopamine (30 μM) application inhibited the same POMC neurons (Fig. 3e,f). Next we tested whether ARC TH cells were in synaptic contact with AgRP neurons. In 11 AgRP neurons in slices containing TH axons expressing ChIEF, we found no synaptic responses to photostimulation, suggesting that dopamine innervation of NPY/AgRP neurons may arise elsewhere, or that excitation of NPY/AgRP cells could occur via nonsynaptic bulk diffusion as described in other systems[21–23].

Arcuate TH neurons inhibit paraventricular nucleus neurons

Previous work on ARC TH cells has focused almost exclusively on axonal projections to the median eminence, where dopamine is released to control pituitary prolactin synthesis[24]. We show here for the first time, to our knowledge, that ARC TH cells not only synapse on POMC neurons (see above) but also maintain a substantial inhibitory projection to the hypothalamic paraventricular nucleus (PVN), an area implicated in energy homeostasis[5,7] (Fig. 4a–c and Supplementary Fig. 8a). Both photostimulation (20 Hz) and DA (30 μM) hyperpolarized PVN neurons and reduced spike frequency (Fig. 4d,e). Consistent with this observation, stimulation of the many ARC TH ChIEF-expressing axons surrounding PVN neurons (Supplementary Fig. 7b) evoked inhibitory postsynaptic currents in most PVN cells tested (27 of 34) (Fig. 4f–i). Neurotransmitters such as GABA can be released by single action potentials, whereas neuromodulators such as dopamine often depend on bursts of spikes to enhance release[25]. Notably, trains of optogenetic stimuli evoked a sustained outward current in the PVN that was dependent on both $GABA_A$ and dopamine receptor activation (Fig. 4j–k and Supplementary Fig. 9). The amplitude of the sustained current was attenuated by the D2 receptor antagonist sulpiride and further attenuated by addition of the $GABA_A$ receptor antagonist bicuculline (Fig. 4k), suggesting that inhibition was due to axonal release of both dopamine and GABA during high-frequency stimulation and indicating that the stimulation of ARC TH axons did evoke dopamine release. The inhibitory valence of ARC TH cells is opposite that of the more rostral hypothalamic TH neurons that

were recently reported to evoke excitatory actions in PVN neurons to modulate maternal care and oxytocin release[26].

Dopamine inhibits POMC cells but excites AgRP/NPY neurons

A number of studies have shown that dopamine influences energy homeostasis; this has often been interpreted as related to a hedonic or motivational involvement in feeding[12]. An alternate but not mutually exclusive perspective is that dopamine may more directly participate in modulating energy balance, in part by modulating the activity of two key neurons involved in energy regulation, the ARC anorexigenic POMC neuron and the orexigenic NPY/AgRP neuron. To address this hypothesis, we used cell-attached and whole-cell recording in hypothalamic brain slices. We have previously shown that dopamine can exert either excitatory or inhibitory actions on unidentified ARC neurons[27], consistent with the localization of both D1 and D2 dopamine receptors in different unidentified neurons from the ARC[28]. Here we found that dopamine exerted a substantial, consistent, and direct dose-dependent inhibition of GFP-expressing POMC neurons, hyperpolarizing the membrane potential by 10 mV when applied at 30 μM and reducing spike frequency (Fig. 5a–c). The inhibition was direct and, on the basis of the reversal potential, the inward rectification, and attenuation by both Ba^{2+} and GDP-β-s, was most likely mediated by a G-protein-coupled inwardly rectifying potassium channel (GIRK) current (Supplementary Fig. 10) acting via a D2-like receptor. The D2 agonist quinpirole exerted a similar inhibition whereas the D1 agonist SKF38393 had little effect (Fig. 5a–c). The D2 antagonist sulpiride attenuated and almost eliminated the dopamine-evoked current (Fig. 5d). With immunostaining, we found TH axons targeting POMC neurons (Fig. 5e). In contrast to its inhibitory effect on POMC cells, dopamine excited the AgRP neurons through a D1-like receptor (Fig. 5f–h), and dopamine-immunoreactive axons were found surrounding some NPY/AgRP neurons (Supplementary Fig. 10d). SKF38393 exerted a similar excitation, whereas quinpirole had little effect (Fig. 5f–h). The actions of dopamine on AgRP neurons continued in the presence of GABA and glutamate receptor antagonists (Supplementary Fig. 11a–c), indicating a direct excitatory effect. These data support the potential for dopamine to exert a direct action on hypothalamic neurons that control feeding; inhibition of POMC neurons and excitation of AgRP neurons both suggest an orexigenic action for dopamine in the ARC.

Arcuate TH neurons are excited by hunger

To explore whether ARC TH neurons respond to metabolic conditions, we tested the effect of 24 h food deprivation on the activity of these neurons in TH-tdTomato transgenic mice. Using immunocytochemistry to examine the expression of nuclear c-fos, we found that fasting increased c-fos protein expression in tdTomato-expressing red TH neurons, almost tripling the number of TH neurons with nuclear c-fos (Fig. 6a–e). C-fos was also increased in other unidentified non-TH neurons, consistent with previous reports of hunger-induced c-fos in NPY/AgRP and other hypothalamic neurons; the magnitude of the fasting-induced c-fos effect in TH neurons was similar to that reported in other neurons sensitive to fasting[29–31].

We also compared resting membrane potential and firing rate in ARC TH neurons of 24-h fasted mice and normally fed control mice. Fasting significantly depolarized the resting membrane potential of TH neurons by 7.5 mV and substantially increased the firing rate by 206% (Fig. 6f–h). These results together support the view that ARC TH neurons are sensitive to cues of energy homeostasis and that both gene expression (c-fos) and electrical activity are increased in states of food deprivation.

Ghrelin excites arcuate TH neurons

If ARC TH neurons modulate energy homeostasis, then they may respond to long-distance signals from the gut. Ghrelin is released from the stomach when the gut is empty and signals the brain to increase energy stores[32,33]. To record selectively from TH neurons, we used a transgenic mouse in which tdTomato was expressed as a red fluorescent reporter under control of the TH promoter, described elsewhere[15]. Ghrelin exerted a direct excitatory action on ARC TH cells (Fig. 7), depolarizing the membrane potential and evoking an inward current. The depolarizing response was not blocked by tetrodotoxin or by GABA and glutamate receptor antagonists (Supplementary Fig. 12), indicating the response was direct rather than synaptically mediated from other cells. The majority of TH neurons in the dorsomedial ARC contain dopamine and display burst firing patterns[15,34]; ghrelin reduced the inter-burst interval, depolarized the membrane potential, increased spike frequency, and generated burst-firing in quiet cells (Fig. 7f–h and Supplementary Fig. 12). The distinctive electrophysiological characteristics of TH neurons, particularly the regular burst pattern of action potentials found in the majority of recorded dopamine cells, was different from the physiological characteristics of POMC and NPY/AgRP cells recorded above, further substantiating the view that the TH cells constitute a population of ARC neurons that are distinct from other ARC neurons.

DISCUSSION

The ARC TH cell not only maintains local axon collaterals to other ARC neurons that control feeding, but also projects dorsally into the PVN to exercise an additional level of regulation of neurons that modulate energy homeostasis and feeding. The majority of PVN axons tested near positive TH axons showed an inhibitory response to optogenetic stimulation of the TH neurons, underlining the strength of the projection. PVN neurons play a key role in the efferent projection of the orexigenic NPY/AgRP neurons[5,35], and our data show a parallel circuit for the ARC TH neuron. Consistent with findings from Golgi impregnations[36], axons from TH cells exit the ARC to innervate not only the PVN, but also the hypothalamic ventromedial and dorsomedial nuclei, regions of the CNS that are also involved in energy homeostasis.

A substantial body of work has focused on extrahypothalamic TH neurons, particularly from the midbrain, that release dopamine and influence feeding[13]. Our data do not contradict that work, but suggest that an additional system involving the ARC TH cell may directly contribute to hypothalamic energy homeostasis by sensing long-distance energy-related signals and directly modulating the activity of several key cell types within the ARC and PVN feeding circuits by releasing both dopamine and the inhibitory amino acid transmitter

GABA (Supplementary Fig. 13). Depending on the dopamine receptor subtype of the targeted cell, dopamine can either inhibit—for example, by acting at a D2-like receptor on POMC or PVN neurons— or excite other cells; for instance by activating a D1-like receptor on AgRP/NPY cells. Thus, the opposing electrophysiological actions of dopamine on POMC and NPY/AgRP cells are both consistent with a direct orexigenic action of dopamine in the ARC. Furthermore, dopamine signaling can alter the gene expression of both POMC[37] as well as NPY and AgRP[38]. Finally, as the ARC maintains a leaky blood brain barrier[36,39], blood-borne signals reflecting nutrient state may more easily access TH neurons here than in other regions of the brain such as the ventral tegmental area which can also respond to signaling cues related to metabolic state[40,41]. The dopamine responses of NPY/AgRP and POMC neurons suggest that dopamine neurons outside the ARC might also contribute to the modulation of these two cell types to influence food intake. In contrast to the more global widespread contribution of the extrahypothalamic dopamine system to the hedonic aspect of feeding, the ARC dopamine cells appear to be more directly involved in modulation of the feeding circuits of the hypothalamus.

The behavioral results showing an optogenetically evoked increase in food intake and a TeNT-mediated reduction in body weight and weight gain are consistent with an orexigenic role for the ARC TH cell, based on stimulation or inhibition of many but not all ARC TH neurons, as determined by histological verification. Recruitment of all ARC TH neurons may generate a greater effect.

We found that food deprivation increased c-fos expression in the ARC TH neurons, as well as in other, unidentified neurons. In addition, whole cell recording showed that hunger depolarized the resting membrane potential and increased the frequency of action potentials, further corroborating the perspective that these cells monitor long distance signals of nutrient state and that conditions of reduced food availability increase TH neuron electrical activity. The long-distance signal peptide ghrelin from the stomach evokes a strong direct excitatory action on ARC TH cells. One physiological characteristic of many ARC dopamine cells is the regular burst firing[15,34], not generally found in other types of ARC neurons and potentially related to enhanced transmitter release. Ghrelin increased burst firing, consistent with the view that these neurons directly monitor and respond to long distance signals of energy homeostasis.

Many TH neurons in the ARC contain immunoreactive dopamine[15] and the GABA-synthesizing enzyme glutamate decarboxylase[20], and can release both GABA and dopamine. Not all TH neurons in the mouse ARC contain dopamine[15]. ARC TH cells that show no detectable dopamine may contain growth hormone releasing hormone (GHRH), which, like dopamine, can be released in the median eminence; the TH neurons also contain other neuropeptides[42,43]. We cannot exclude the possibility that these non-dopamine TH cells also participate in energy homeostasis, potentially related to their primary role in enhancing body size through stimulation of pituitary growth hormone release by GHRH. Like other neurons that regulate energy homeostasis, TH neurons release both slow neuromodulators, such as dopamine, and also a fast amino acid transmitter, GABA. This allows the potential for multiple permutations of responses in different cells postsynaptic to TH axons.

The NPY/AgRP neuron can increase feeding[5,10], and dopamine does excite the NPY/AgRP neuron; however, ARC TH neurons do not appear to act simply by exciting the NPY/AgRP neurons, since we found no detectable direct synaptic action of ARC TH neurons on NPY/AgRP neurons and no colocalization of TH in NPY/AgRP cells. By contrast, anorexigenic POMC cells were inhibited directly by GABA release from ARC TH neurons. Inhibitory modulation of POMC cells may contribute to the extended actions of TH cells in energy homeostasis, including the long-term weight reduction found with TH cell TeNT-mediated attenuation, but they probably do not bear a primary responsibility for the optogenetically induced orexigenic actions. Previous work suggested that ARC POMC neurons contribute to long-term reduction in food intake, but are not responsible for shortterm rapid control of feeding[10,44]. Together these electrophysiological, neuroanatomical, optogenetic, and behavioral data suggest that ARC TH neurons can act independently and/or in concert with other ARC neurons to regulate energy homeostasis and enhance food intake.

ONLINE METHODS

Animals.

Mice were housed in a climate-controlled environment at 22 °C with a 12 h/12 h light/dark cycle and *ad libitum* access to standard mouse lab pellet food and water. All animals and procedures in this study were approved by the Yale University Committee on Animal Care and Use. TH-tdTomato transgenic mice were generated and provided by Gensat/Rockefeller University, and were recently characterized[15]. TH-Cre mice were a gift from R. Greene, J. Zigman, T. Dawson, and J. Savitt[45]. POMC-GFP mice[8] (gift of M. Low) and NPY-GFP mice (gift of B. Lowell)[46] have been described previously. A total of 179 mice (108 male and 71 female) were used in the experiments. Many of the transgenic lines were outcrossed to Swiss Webster mice. The mice were group-housed except for those mice used for optogenetic behavior study mentioned below.

Virus vector injection and fiber implantation.

TH-Cre mice (6–8 weeks old) were anesthetized with xylazine (20 mg/kg) and ketamine (100 mg/kg) and placed into a stereotaxic apparatus (David Kopf Instruments CA, USA). After exposing the skull via a small incision, a small hole was drilled for injection. A pulledglass pipette with a 20–40 μm tip diameter was beveled and inserted into the ARC (coordinates, bregma: AP: −1.30 mm, DV: −5.90 mm, L: −0.20 mm) and Cre-dependent adeno-associated virus (AAV)dj-CAG-DIO-ChIEF-tdTomato (25–100 nl) or (AAV)dj-CAG-DIO-TeNT-GFP (both from Stanford University Viral Vector Core) (25–100 nl) was bilaterally injected using a motorized stereotaxic injector (model 7803115, Stoelting Co., IL, USA) that controlled a Hamilton syringe connected to the glass pipette to generate an injection rate of 30 nl per min, and the pipette was slowly withdrawn 10 min after injection. Immediately after withdrawal of the injection pipette, an optical fiber (200 μm core, NA 0.22, Doric lenses, Canada) was inserted into the hypothalamus and the fiber tip was placed above the ARC. The coordinates for the fiber tip were AP: −1.30 mm, DV: −5.5 mm, L: −0.10 mm. Mice with fiber implants were singly housed for 3 weeks of recovery before any electrophysiology or behavior experiments.

Slice electrophysiology.

Slices were obtained from transgenic TH- tdTomato (P14–60), POMC-GFP (P14–60), NPY-GFP (P14–P60) and ChIEF-tdTomato (at least 21 d after virus injection) mice. On the day of the experiment, mice were anesthetized with isoflurane and decapitated. Brains were immersed in ice-cold high-sucrose solution containing (in mM) 220 sucrose, 2.5 KCl, 6 $MgCl_2$, 1 $CaCl_2$, 1.23 NaH_2PO_4, 26 $NaHCO_3$, and 10 glucose (gassed with 95% O_2/5% CO_2; 300–305 mOsm). Coronal brain slices containing the hypothalamus (300 μm thick) were prepared using a vibratome. Brain slices were transferred to an incubation chamber containing artificial CSF (ACSF) solution containing (in mM) 124 NaCl, 2.5 KCl, 2 $MgCl_2$, 2 $CaCl_2$, 1.23 NaH_2PO_4, 26 $NaHCO_3$, and 10 glucose (gassed with 95% O_2/5% CO_2; 300–305 mOsm) and incubated at room temperature (22 °C). After a 1–2 h recovery period, slices were transferred to a recording chamber mounted on a BX51WI upright DIC/fluorescence microscope (Olympus, Tokyo, Japan) and perfused with a continuous flow of gassed ACSF. Experiments were performed at 33 ± 1 °C using a dual-channel heat controller (Warner Instruments, Hamden, CT).

Cell-attached and whole-cell patch-clamp recordings were performed on fluorescent ARC neurons and unidentified PVN neurons that were visualized using an infrared differential interference contrast (DIC) optical system combined with a CCD camera and monitor. Pipettes used for recording were pulled from thin-walled borosilicate glass capillary tubes (length 75 mm, outer diameter 1.5 mm, inner diameter 1.1 mm, World Precision Instruments, Sarasota, FL) using a P-97 Flaming/Brown micropipette puller (Sutter Instruments, Novato, CA). Pipette solution contained (in mM) 145 potassium gluconate, 1 $MgCl_2$, 10 HEPES, 1.1 EGTA, 2 Mg-ATP, 0.5 Na_2-GTP, and 5 Na_2-phosphocreatine (pH 7.3 with KOH; 290–295 mOsm). Pipettes with resistances ranging from 4 to 6 MΩ were selected for recording. An EPC-10 patch-clamp amplifier (HEKA Instruments, Bellmore, NY) and PatchMaster 2.20 software (HEKA Elektronik, Lambrecht/Pfalz, Germany) were used to acquire and analyze data. Neurons in which the series resistance was >20 MΩ and changed >15% during recording were excluded from analysis. Traces were processed using Igor Pro 6.36 (Wavemetrics, Lake Oswego, OR). Inhibitory postsynaptic currents were analyzed with MiniAnalysis 6.03 (Synaptosoft Inc., Decatur, GA). For optogenetic stimulation of ChIEF channels in brain slices, an LED array (BXRAC2002, Bridgelux, Livermore, CA) was used. Duration (10 ms) and frequency (single stimulation or 1, 5, 10 or 20 Hz) of stimulation were set with a Grass S44 stimulator (Natus Neurology, Warwick, RI).

Immunocytochemistry.

To confirm that tdTomato or ChIEF-tdTomato was expressed in TH neurons of TH-tdTomato mice or TH-Cre mice injected with AAV Cre-dependent ChIEF-tdTomato, we combined detection of green immunofluorescence with detection of tdTomato (red fluorescence) in TH-tdTomato mice or TH-Cre mice injected with Cre-dependent ChIEF-tdTomato-AAV. Mice were anesthetized with Euthasol and then perfused transcardially with saline followed by 4% paraformaldehyde or 3% glutaraldehyde. Coronal sections 16 μm thick were cut on a cryostat, immersed in phosphate-buffered saline (PBS) for 1 h, treated with 2% normal horse serum in PBS for 1 h, and then incubated overnight at 4 °C in rabbit anti-TH (Millipore, AB152, 1:5,000)[15] or anti-dopamine antiserum (from H. Steinbusch, 1:1,000) described in

detail elsewhere[19,47]. After washing in PBS, sections were placed in secondary goat anti-rabbit Alexa488 (Abcam, AB150073, 1:500) or Alexa594-conjugated donkey anti-rabbit IgG (Life Technologies, A21207, 1:250) for 2 h, washed, and mounted on glass slides. Sections were studied on an Olympus IX70 inverted fluorescence microscope. Micrographs were recorded with a SPOT digital camera (Diagnostic Instruments, Sterling Heights, MI), and contrast and brightness were corrected using Photoshop.

Food intake analysis.

Mice had *ad libitum* access to mouse chow in the home cage before and after the optogenetic food intake test. For food intake tests, measured from 11:00 to 14:00 each day, mice were connected to a 473-nm blue laser and transferred into a transparent cage for 1 h to measure food intake. Prior to data acquisition, mice were singly housed and habituated for 1 h to the test cage at the same time each day. After the 1-h food intake baseline was stable, 1 h of food intake was tested in control and ChIEF-expressing mice with photostimulation. In the control group, AAV-GFP was injected into the ARC of TH-Cre mice to induce GFP expression in ARC TH neurons in the absence of ChIEF expression.

Light was delivered to the brain through an optical fiber from a 473-nm blue laser (Doric Lenses, Canada). To connect the fiber to the cannula on the skull, mice were briefly anesthetized with isoflurane the day before photostimulation. The stimulus (10 ms duration) was applied repeatedly over 2 s with different frequencies followed by 3 s off, with this sequence repeated 720 times. To observe the frequency-dependent effect of photostimulation on food intake, 5, 10, 20 Hz were applied in the study.

Body weight.

Fifteen male TH-Cre mice were divided into two groups, with each group having the same mean initial body weight for the body weight gain experiment. The mice had been outbred to a Swiss Webster background. Swiss Webster mice are large and normally have body weights almost twice the body weight of some inbred strains of mice. A control group of 7 male mice was injected with AAV-GFP in ARC and 8 male mice were injected with an AAV expressing the Cre-dependent synaptic silencer TeNT in ARC. The week before surgery, mice were weighed to obtain a body weight baseline. After surgery, we measured the body weight for each mouse once a week for more than half a year. The body weight gain was obtained by calculating the percentage of increased body weight compared to the baseline level the week before surgery.

c-fos expression and neuron activity analysis after fasting.

TH-tdTomato transgenic mice from the same litters were divided into two groups and were acclimated to handling for 10 d before food deprivation. The day before the experiment, control mice received food *ad libitum* whereas fasted mice were deprived of food for 24 h. The mice were given an anesthetic overdose and perfused with fixative, and brains were sectioned as described above. The same fasting procedure was also used to record neuron activity electrophysiologically. Fresh slices from both normally fed mice and 24-h fasted mice were collected for patch clamp recording of resting membrane potential and firing rate of TH neurons.

For c-fos immunostaining, the brain sections were washed and incubated in rabbit anti-c-fos (Oncogene, PC38, 1:3000) overnight; the antibody is characterized elsewhere[29]. After additional washes to remove the primary antiserum, sections were incubated in goat anti-rabbit Alexa488 (Abcam, AB150073, 1:500) for 2 h, washed, and then mounted on glass slides. The number of red TH neurons that expressed green c-fos immunoreactivity in the cell nucleus was determined using an Olympus IX70 fluorescent microscope.

Drugs and drug application.

Ghrelin (rat, mouse) was purchased from Phoenix Pharmaceuticals (Burlingame, CA). Tetrodotoxin (TTX), bicuculline (Bic), 6-cyano-7-nitroquinoxaline-2,3-dione (CNQX) and d-2-amino-5-phosphonopentanoic acid (AP5), quinpirole, SKF38393 and sulpiride were from Tocris Bioscience (Ellisville, MO). Dopamine was from Sigma-Aldrich (St. Louis, MO). Drugs were prepared and stored as stock solutions according to the manufacturer's instructions and diluted in ACSF to obtain the experimental concentrations used in each experiment. All drug solutions were administered by a large-diameter (300 μm) flow pipe with the tip directed toward the recorded cell. During periods of no drug application, normal ACSF was continuously supplied to the recorded cell through the flow pipe.

Overall experimental design and analysis.

No statistical methods were used to predetermine sample sizes; our sample sizes are similar to those generally employed in the field. Animals were randomly assigned to the different experimental groups except for the body weight gain experiment, where mice were assigned to each group to generate equivalent initial group body weights. Data collection and analysis were not performed blind to the conditions of the experiments. Data points were not excluded from analysis except for the behavior experiments when histological analysis showed no ChIEF or TeNT expression. Individual data points are shown in the figures and data distribution was assumed to be normal but this was not formally tested.

Statistical analysis.

Data are expressed as mean ± s.e.m. Group statistical significance was assessed using two-sided Student's *t* test for comparison of two groups, and one-way or two-way ANOVA followed by a Bonferroni *post hoc* test for three or more groups. $P < 0.05$ was considered statistically significant.

A **Supplementary Methods Checklist** is available.

Data availability.

The data supporting the findings of this study are available from the authors upon request.

Supplementary Material

Refer to Web version on PubMed Central for supplementary material.

ACKNOWLEDGMENTS

We thank D. Spergel, J. Paglino and J. Davis for manuscript suggestions; I. Araujo and W. Han for suggestions on behavioral optogenetics; Y. Yang for technical assistance; R. Greene (UT Southwestern) and J. Zigman, T. Dawson, J. Savitt (Johns Hopkins University) for TH-Cre mice; M. Low (University Michigan) for POMC-GFP mice; and B. Lowell (Harvard University) for NPY-GFP mice. We thank H. Steinbusch (Maastricht University) for the dopamine antibody. Support provided by NIH DK084052, DK103176, and NS79274 (A.N.v.d.P.).

References

1. Flier JS Obesity wars: molecular progress confronts an expanding epidemic. Cell 116, 337–350 (2004). [PubMed: 14744442]
2. Schwartz MW, Woods SC, Porte D, Jr., Seeley RJ & Baskin DG Central nervous system control of food intake. Nature 404, 661–671 (2000). [PubMed: 10766253]
3. Grill HJ, Ginsberg AB, Seeley RJ & Kaplan JM Brainstem application of melanocortin receptor ligands produces long-lasting effects on feeding and body weight. J. Neurosci. 18, 10128–10135 (1998). [PubMed: 9822766]
4. Saper CB, Chou TC & Elmquist JK The need to feed: homeostatic and hedonic control of eating. Neuron 36, 199–211 (2002). [PubMed: 12383777]
5. Atasoy D, Betley JN, Su HH & Sternson SM Deconstruction of a neural circuit for hunger. Nature 488, 172–177 (2012). [PubMed: 22801496]
6. Balthasar N et al. Divergence of melanocortin pathways in the control of food intake and energy expenditure. Cell 123, 493–505 (2005). [PubMed: 16269339]
7. Shah BP et al. MC4R-expressing glutamatergic neurons in the paraventricular hypothalamus regulate feeding and are synaptically connected to the parabrachial nucleus. Proc. Natl. Acad. Sci. USA 111, 13193–13198 (2014). [PubMed: 25157144]
8. Cowley MA et al. Leptin activates anorexigenic POMC neurons through a neural network in the arcuate nucleus. Nature 411, 480–484 (2001). [PubMed: 11373681]
9. Tong Q, Ye CP, Jones JE, Elmquist JK & Lowell BB Synaptic release of GABA by AgRP neurons is required for normal regulation of energy balance. Nat. Neurosci. 11, 998–1000 (2008). [PubMed: 19160495]
10. Aponte Y, Atasoy D & Sternson SM AGRP neurons are sufficient to orchestrate feeding behavior rapidly and without training. Nat. Neurosci 14, 351–355 (2011). [PubMed: 21209617]
11. Luquet S, Perez FA, Hnasko TS & Palmiter RD NPY/AgRP neurons are essential for feeding in adult mice but can be ablated in neonates. Science 310, 683–685 (2005). [PubMed: 16254186]
12. Baldo BA & Kelley AE Discrete neurochemical coding of distinguishable motivational processes: insights from nucleus accumbens control of feeding. Psychopharmacology (Berl.) 191, 439–459 (2007). [PubMed: 17318502]
13. Palmiter RD Is dopamine a physiologically relevant mediator of feeding behavior? Trends Neurosci. 30, 375–381 (2007). [PubMed: 17604133]
14. Wise RA Role of brain dopamine in food reward and reinforcement. Phil. Trans. R. Soc. Lond. B 361, 1149–1158 (2006). [PubMed: 16874930]
15. Zhang X & van den Pol AN Dopamine/tyrosine hydroxylase neurons of the hypothalamic arcuate nucleus release GABA, communicate with dopaminergic and other arcuate neurons, and respond to dynorphin, met-enkephalin, and oxytocin. J. Neurosci 35, 14966–14982 (2015). [PubMed: 26558770]
16. Fenno LE et al. Targeting cells with single vectors using multiple-feature Boolean logic. Nat. Methods 11, 763–772 (2014). [PubMed: 24908100]
17. Lin JY, Lin MZ, Steinbach P & Tsien RY Characterization of engineered channelrhodopsin variants with improved properties and kinetics. Biophys. J 96, 1803–1814 (2009). [PubMed: 19254539]
18. Xu W & Südhof TC A neural circuit for memory specificity and generalization. Science 339, 1290–1295 (2013). [PubMed: 23493706]

19. Zoli M, Agnati LF, Tinner B, Steinbusch HW & Fuxe K Distribution of dopamine-immunoreactive neurons and their relationships to transmitter and hypothalamic hormone-immunoreactive neuronal systems in the rat mediobasal hypothalamus. A morphometric and microdensitometric analysis. J. Chem. Neuroanat 6, 293–310 (1993). [PubMed: 7506039]
20. Everitt BJ, Hökfelt T, Wu JY & Goldstein M Coexistence of tyrosine hydroxylase-like and gamma-aminobutyric acid-like immunoreactivities in neurons of the arcuate nucleus. Neuroendocrinology 39, 189–191 (1984). [PubMed: 6147773]
21. Goto Y, Otani S & Grace AA The yin and yang of dopamine release: a new perspective. Neuropharmacology 53, 583–587 (2007). [PubMed: 17709119]
22. Gonon FG Nonlinear relationship between impulse flow and dopamine released by rat midbrain dopaminergic neurons as studied by in vivo electrochemistry. Neuroscience 24, 19–28 (1988). [PubMed: 3368048]
23. Taylor IM, Ilitchev AI & Michael AC Restricted diffusion of dopamine in the rat dorsal striatum. ACS Chem. Neurosci 4, 870–878 (2013). [PubMed: 23600442]
24. Fitzgerald P & Dinan TG Prolactin and dopamine: what is the connection? A review article. J. Psychopharmacol 22 (Suppl.): 12–19 (2008). [PubMed: 18477617]
25. van den Pol AN Neuropeptide transmission in brain circuits. Neuron 76, 98–115 (2012). [PubMed: 23040809]
26. Scott N, Prigge M, Yizhar O & Kimchi T A sexually dimorphic hypothalamic circuit controls maternal care and oxytocin secretion. Nature 525, 519–522 (2015). [PubMed: 26375004]
27. Belousov AB & van den Pol AN Dopamine inhibition: enhancement of GABA activity and potassium channel activation in hypothalamic and arcuate nucleus neurons. J. Neurophysiol 78, 674–688 (1997). [PubMed: 9307104]
28. Romero-Fernandez W et al. Dopamine D1 and D2 receptor immunoreactivities in the arcuate-median eminence complex and their link to the tubero-infundibular dopamine neurons. Eur. J. Histochem 58, 2400 (2014). [PubMed: 25308843]
29. Liu T et al. Fasting activation of AgRP neurons requires NMDA receptors and involves spinogenesis and increased excitatory tone. Neuron 73, 511–522 (2012). [PubMed: 22325203]
30. Yan C et al. Apolipoprotein A-IV inhibits AgRP/NPY neurons and activates POMC neurons in the arcuate nucleus. Neuroendocrinology 10.1159/000439436 (2016).
31. Groessl F, Jeong JH, Talmage DA, Role LW & Jo YH Overnight fasting regulates inhibitory tone to cholinergic neurons of the dorsomedial nucleus of the hypothalamus. PLoS One 8, e60828 (2013). [PubMed: 23585854]
32. Kojima M et al. Ghrelin is a growth-hormone-releasing acylated peptide from stomach. Nature 402, 656–660 (1999). [PubMed: 10604470]
33. Tschöp M, Smiley DL & Heiman ML Ghrelin induces adiposity in rodents. Nature 407, 908–913 (2000). [PubMed: 11057670]
34. Lyons DJ, Horjales-Araujo E & Broberger C Synchronized network oscillations in rat tuberoinfundibular dopamine neurons: switch to tonic discharge by thyrotropinreleasing hormone. Neuron 65, 217–229 (2010). [PubMed: 20152128]
35. Krashes MJ et al. An excitatory paraventricular nucleus to AgRP neuron circuit that drives hunger. Nature 507, 238–242 (2014). [PubMed: 24487620]
36. van den Pol AN & Cassidy JR The hypothalamic arcuate nucleus of rat—a quantitative Golgi analysis. J. Comp. Neurol 204, 65–98 (1982). [PubMed: 7056889]
37. Matera C & Wardlaw SL Dopamine and sex steroid regulation of POMC gene expression in the hypothalamus. Neuroendocrinology 58, 493–500 (1993). [PubMed: 8115018]
38. Kobayashi M et al. Simultaneous absence of dopamine D1 and D2 receptormediated signaling is lethal in mice. Proc. Natl. Acad. Sci. USA 101, 11465–11470 (2004). [PubMed: 15272078]
39. Broadwell RD & Brightman MW Entry of peroxidase into neurons of the central and peripheral nervous systems from extracerebral and cerebral blood. J. Comp. Neurol 166, 257–283 (1976). [PubMed: 57126]
40. Abizaid A et al. Ghrelin modulates the activity and synaptic input organization of midbrain dopamine neurons while promoting appetite. J. Clin. Invest 116, 3229–3239 (2006). [PubMed: 17060947]

41. Naleid AM, Grace MK, Cummings DE & Levine AS Ghrelin induces feeding in the mesolimbic reward pathway between the ventral tegmental area and the nucleus accumbens. Peptides 26, 2274–2279 (2005). [PubMed: 16137788]

42. Everitt BJ et al. The hypothalamic arcuate nucleus-median eminence complex: immunohistochemistry of transmitters, peptides and DARPP-32 with special reference to coexistence in dopamine neurons. Brain Res. 396, 97–155 (1986). [PubMed: 2874874]

43. Meister B et al. Coexistence of tyrosine hydroxylase and growth hormone-releasing factor in a subpopulation of tubero-infundibular neurons of the rat. Neuroendocrinology 42, 237–247 (1986). [PubMed: 2869425]

44. Zhan C et al. Acute and long-term suppression of feeding behavior by POMC neurons in the brainstem and hypothalamus, respectively. J. Neurosci 33, 3624–3632 (2013) [PubMed: 23426689]

45. Savitt JM, Jang SS, Mu W, Dawson VL & Dawson TM Bcl-x is required for proper development of the mouse substantia nigra. J. Neurosci 25, 6721–6728 (2005). [PubMed: 16033881]

46. van den Pol AN et al. Neuromedin B and gastrin-releasing peptide excite arcuate nucleus neuropeptide Y neurons in a novel transgenic mouse expressing strong Renilla green fluorescent protein in NPY neurons. J. Neurosci 29, 4622–4639 (2009). [PubMed: 19357287]

47. van den Pol AN, Herbst RS & Powell JF Tyrosine hydroxylase-immunoreactive neurons of the hypothalamus: a light and electron microscopic study. Neuroscience 13, 1117–1156 (1984). [PubMed: 6152034]

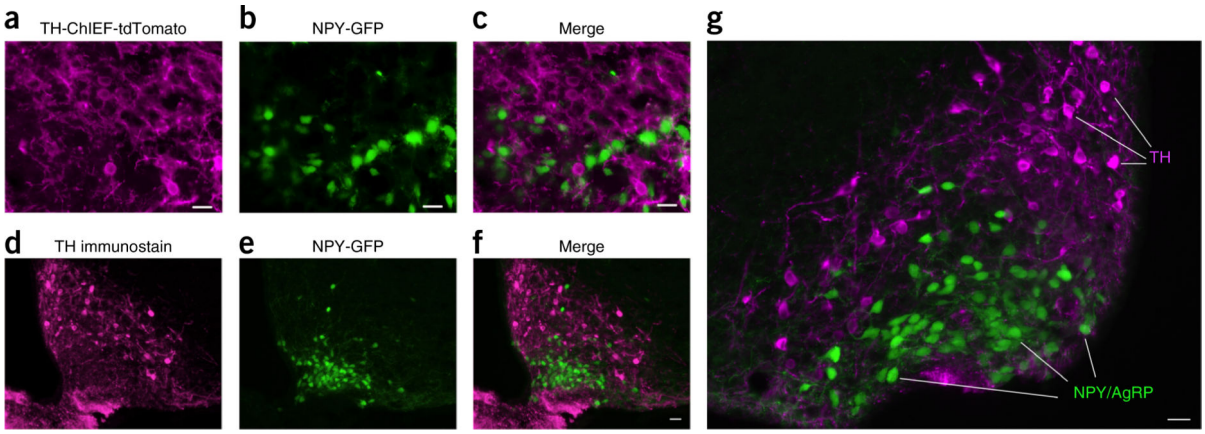

Figure 1.

Lack of colocalization of TH in NPY/AgRP neurons. (**a**) TH-ChIEF-tdTomato neurons are shown in magenta after Cre-dependent AAV-ChIEF-tdTomato (arrows) was injected into ARC of a TH-Cre mouse crossed with an NPY-GFP mouse. (**b**) NPY-GFP neurons are shown in the ARC on the same section as in **a**. (**c**) Merged image shows that TH neurons do not overlap with NPY/AgRP cells. Scale bar, 20 μm. We analyzed 45 sections from 3 mice with a combination of low and high magnification fluorescence microscopy; 1,561 TH-ChIEF-tdTomato expressing cells were identified and none expressed the NPY/AgRP GFP. Similarly, 2,756 NPY/AgRP-GFP expressing cells were examined and none expressed detectable TH-ChIEF-tdTomato. (**d**) Arcuate TH immunostained cells are shown in magenta from an NPY-GFP transgenic mouse. (**e**) Green neurons are shown from the same section of the NPY-GFP transgenic mouse in **d**. (**f**) Merged image reveals no overlap between magenta TH-ChIEF-tdTomato and green NPY/AgRP neurons. Scale bar, 20 μm. (**g**) Higher magnification of a similar merged image is shown from another section. 18 sections from [3]NPY-GFP mice were examined. Scale bar, 20 μm.

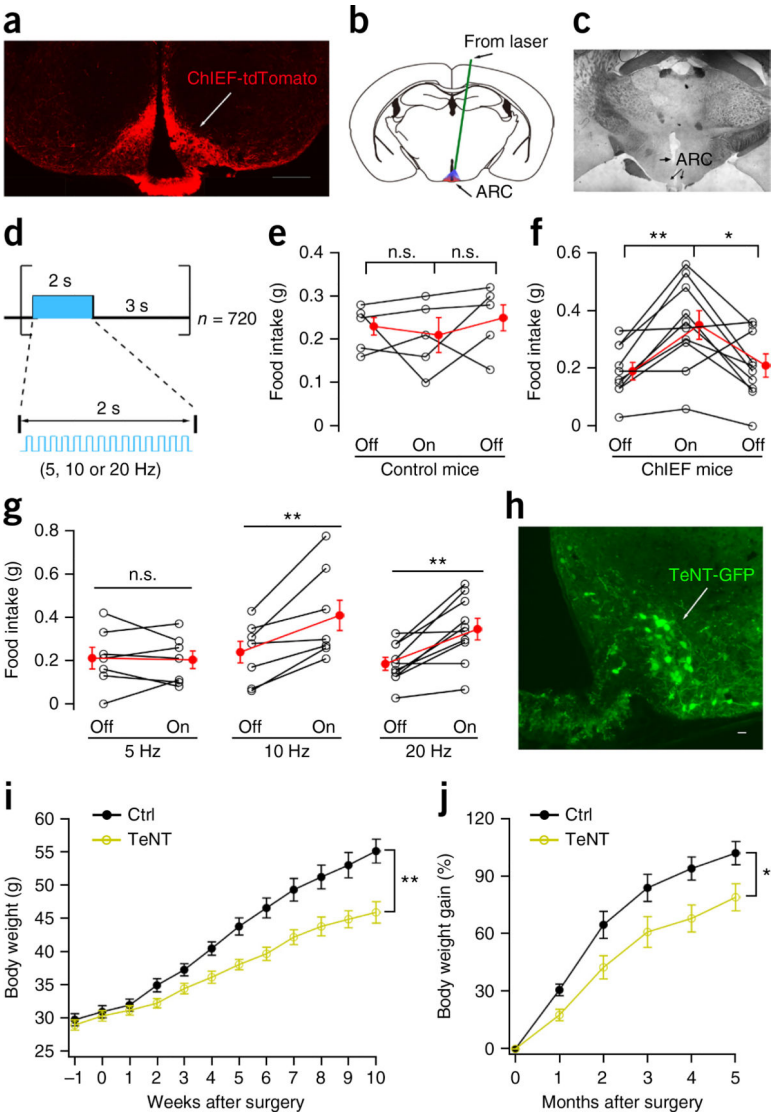

Figure 2.

Arcuate TH neurons enhance food intake and body weight gain. (**a**) Restricted expression of ChIEF-tdTomato in ARC after AAV Cre-dependent ChIEF-tdTomato was injected into both sides of ARC in TH-Cre mice. Scale bar, 400 μm. (**b**) The implanted optical fiber tip was 0.5 mm above the ARC. (**c**) Histology; arrow denotes fiber tip. (**d**) Photostimulation for 1 h with 2 s laser on (5, 10 or 20 Hz) followed by 3 s laser off, repeated 720 times. (**e**) Food intake for control ($n = 5$ mice) without ChIEF during 1 h of no stimulation (off) and 1 h photostimulation (on) at 20 Hz, followed by 1 h of no stimulation (off). Food measured from 11:00 to 14:00. One-way repeated measures ANOVA, $F(4,8) = 2.787$, $P = 0.101$. Mean ± s.e.m. (red). (**f**) Food intake ($n = 10$ mice) with ChIEF in ARC TH neurons during 1 h of no stimulation (off) and 1 h photostimulation (on) at 20 Hz. One-way repeated measures ANOVA, $F(9,18) = 4.98$, $P = 0.002$. Light-on versus light off: $^{*}P = 0.035$, $^{**}P = 0.045$, Bonferroni *post hoc* comparison. Mean ± s.e.m. (red). (**g**) Mean food intake with ChIEF expression during 1 h of no stimulation and 1 h photostimulation at 5 ($n = 7$ mice), 10 ($n = 7$ mice) and 20 Hz ($n = 10$ mice). For paired two-tailed *t* test: $t(6) = 0.279$, $t(6) = 3.757$, $t(6) =$

4.494 for 5 Hz, 10 Hz and 20 Hz respectively. Stimulus on versus off: $P = 0.791$, $P = 0.009$, $P = 0.002$ for 5 Hz, 10 Hz, 20 Hz, respectively. Mean ± s.e.m. (red). (**h**) Restricted expression of TeNT-GFP in ARC after AAV Cre-dependent TeNT-GFP injected into ARC in TH-Cre mice. Scale bar, 20 μm. (**i**) Mean body weight (± s.e.m.) for control ($n = 7$ mice) and TeNT ($n = 8$ mice) groups measured after AAV Cre-dependent TeNT-GFP injection. $F(1,13) = 12.24$, $^{**}P = 0.004$, two-way ANOVA. Mice used were on Swiss Webster background. (**j**) Body weight gain from control ($n = 7$ mice) and TeNT group ($n = 8$ mice) during 5 months after AAV Cre-dependent TeNT-GFP injection. Mice with attenuated TH neuron transmitter release showed substantial reduction in body weight (mean ± s.e.m.). $F(1,13) = 6.904$, $^{*}P = 0.021$, two-way ANOVA.

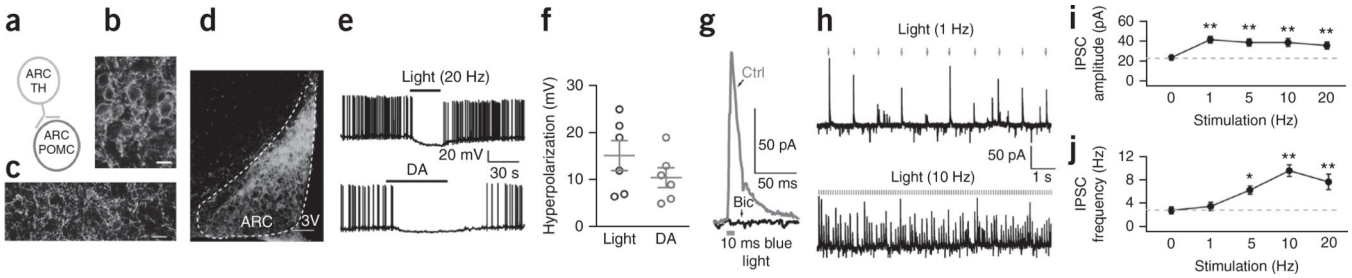

Figure 3.

Hypothalamic arcuate TH neurons inhibit arcuate POMC neurons. (**a**) Connections tested between ARC TH neurons and POMC neurons. (**b**) Photomicrograph showing cell bodies of ChIEF-tdTomato-expressing neurons after AAV Cre-dependent ChIEF-tdTomato microinjection into the ARC of TH-Cre mice. Scale bar, 20 μm. (**c**) Photomicrograph showing local axons arising and terminating in the ARC. Scale bar, 20 μm. (**d**) Restricted ChIEF-tdTomato expression was found in ARC. Scale bar, 90 μm; 3V, third ventricle. A similar fluorescence pattern was observed in 10 mice. (**e**) Blue light (10 ms, 20 Hz) hyperpolarizes and inhibits a GFP-expressing POMC neuron (top trace), and dopamine (DA, 30 μM) inhibits the same neuron (bottom trace). (**f**) Mean hyperpolarization in POMC neurons (± s.e.m.; red) by light or DA (n = 6 cells from 2 mice). (**g**) IPSC evoked by brief 10-ms photostimulation in a POMC neuron, which was abolished by bicuculline (Bic, 30 μM). Holding potential, −40 mV. (**h**) Traces showing high fidelity of IPSCs evoked by 10 ms photostimulation at 1 Hz (top) and high-frequency IPSCs evoked by 10 Hz photostimulation (bottom). (**i**) IPSC amplitude (mean ± s.e.m.) during optogenetic stimulation at different frequencies (n = 10 cells from 4 mice). One-way repeated-measures ANOVA, $F(9,36)$ = 16.71, $P < 0.0001$. By Bonferroni *post hoc* comparison: $P = 0.0005$ for 1 Hz vs. 0 Hz, $P = 0.003$ for 5 Hz vs. 0 Hz, $P = 0.008$ for 10 Hz vs. 0 Hz, $P = 0.009$ for 20 Hz vs. 0 Hz; $^{**}P < 0.01$. (**j**) IPSC frequency during optogenetic stimulation at different frequencies (n = 10 cells from 4 mice). One-way repeated measures ANOVA, $F(9,36) = 5.585$; compared to control without photostimulation by Bonferroni *post hoc* comparison: $P = 0.043$ (5 Hz), $P < 0.0001$ (10 Hz), $P = 0.002$ (20 Hz). Mean ± s.e.m.

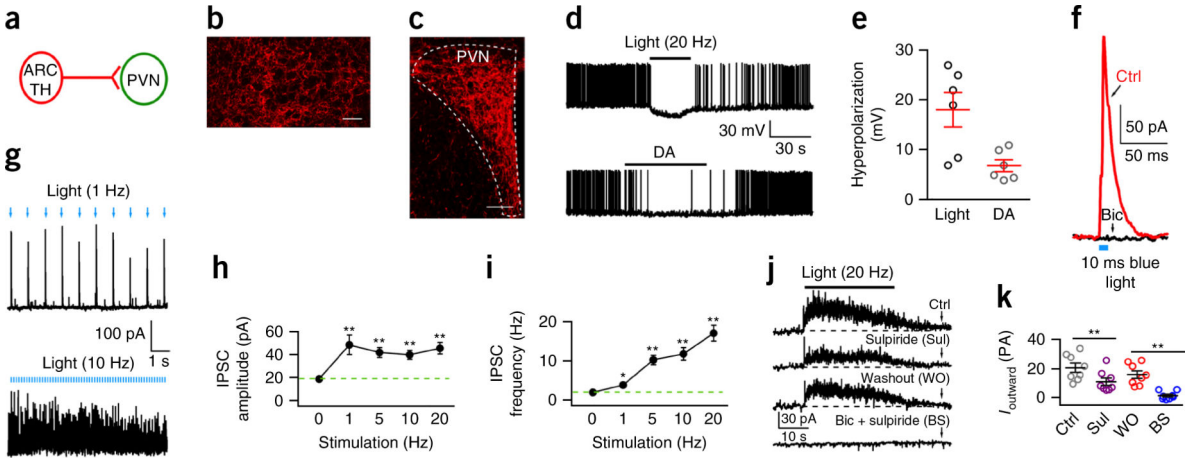

Figure 4.

Hypothalamic ARC TH neurons inhibit PVN neurons. (**a**) Connections tested between ARC TH neurons and PVN neurons. (**b**) High density of ChIEF-tdTomato-expressing axons in PVN after AAV Cre-dependent ChIEF-tdTomato microinjections in ARC of TH-Cre mice. Scale bar, 20 μm. No labeled cell bodies were found in PVN, showing axons arose from ARC. (**c**) Labeled ARC axons innervate PVN. Scale bar, 90 μm. Similar fluorescence was seen in 10 mice. (**d**) Optogenetic stimulation (10 ms, 20 Hz) hyperpolarizes and inhibits a PVN neuron (top trace), and dopamine (DA, 30 μM) inhibits the same neuron (bottom trace). (**e**) Mean hyperpolarization (± s.e.m.; red) induced by both light and DA. (**f**) IPSC evoked by 10 ms photostimulation of a PVN neuron, which was abolished by bicuculline (Bic, 30 μM). Holding potential, −40 mV. (**g**) Traces showing high fidelity of IPSCs evoked by 10 ms photostimulation of 1 Hz (top) and high frequency of IPSCs evoked by 10 ms photostimulation of 10 Hz (bottom). (**h**) Mean (± s.e.m.) IPSC amplitude during photostimulation at different frequencies (n = 8 cells from 4 mice). One-way repeated measures ANOVA, $F(7,28) = 5.46$, $P = 0.0005$; $^{**}P < 0.01$ compared to control without photostimulation by Bonferroni *post hoc* test. (**i**) Mean (± s.e.m.) IPSC frequency during photostimulation at different frequencies (n = 8 from 4 mice). One-way repeated measures ANOVA, $F(7,28) = 2.46$, $P = 0.043$; by Bonferroni *post hoc* test: $P = 0.001$ for 1 Hz vs. 0 Hz, $P = 0.0004$ for 5 Hz vs. 0 Hz, $P = 0.002$ for 10 Hz vs. 0 Hz, $P = 0.0005$ for 20 Hz vs. 0 Hz; $^{**}P < 0.01$. (**j**) Tonic outward current evoked by 20 Hz photostimulation for 30 s, showing control, D2 receptor antagonist sulpiride (10 μM), washout, and bicuculline (30 μM) + sulpiride. (**k**) Means and s.e.m. (n = 8 cells from 4 mice) in **j**. $F(7,21) = 9.51$, $P < 0.0001$, one-way repeated measures ANOVA. By Bonferroni *post hoc* test, $P = 0.001$ for Sul vs. Ctrl, $P = 0.002$ for BS vs. WO; $^{**}P < 0.01$. These data suggest GABA and dopamine are released from TH neurons by optogenetic stimulation, and both contribute to PVN inhibition.

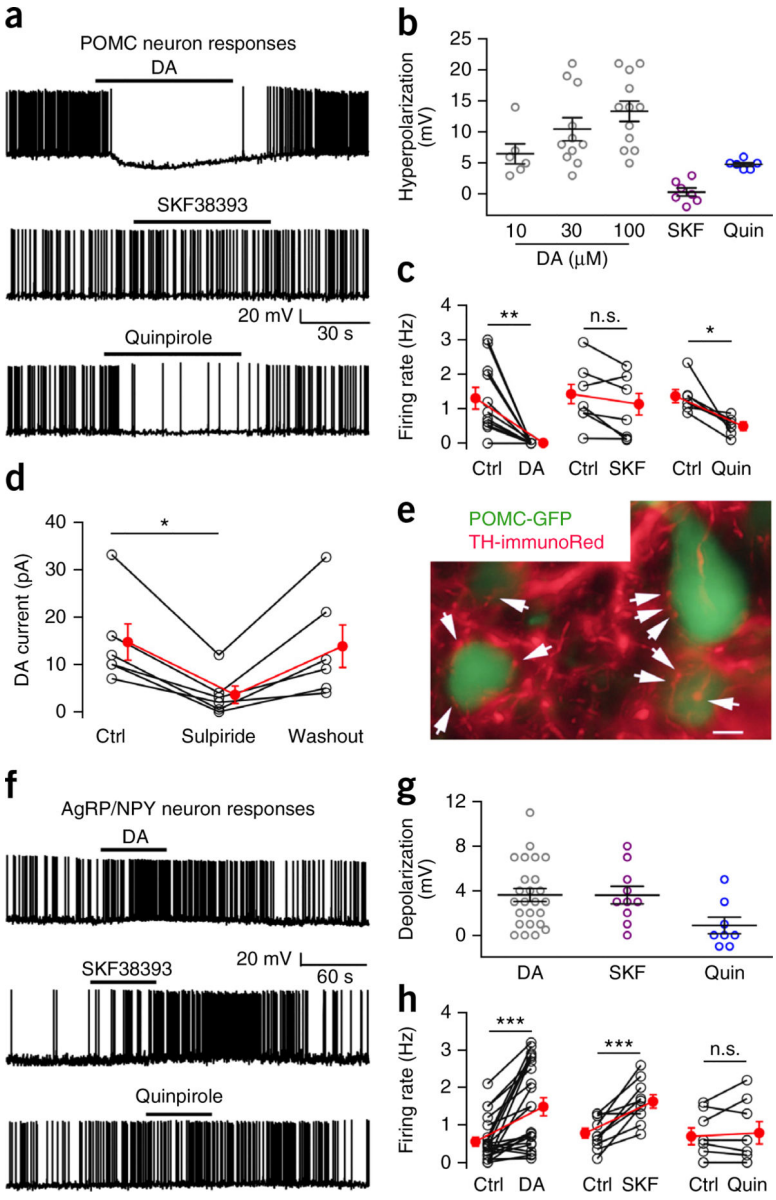

Figure 5.

Dopamine inhibits arcuate POMC neurons but excites NPY/AgRP neurons. (**a**) Dopamine (DA) (top, 30 μM) and D2 receptor agonist quinpirole (Quin) (bottom, 10 μM) inhibit POMC cells. D1 agonist SKF38393 (middle, 10 μM) shows no effect. (**b**) POMC neuron membrane hyperpolarization by DA (10 μM, $n = 6$; 30 μM, $n = 11$; and 100 μM, $n = 12$ cells from 5 mice), SKF38393 ($n = 7$ cells from 4 mice) and quinpirole ($n = 6$ cells from 3 mice). Mean ± s.e.m. (**c**) Firing rate before (control; Ctrl) and with DA (30 μM, $n = 11$ cells from 5 mice), SKF38393 ($n = 7$ cells from 4 mice) and quinpirole ($n = 6$ cells from 3 mice). Paired two-tailed t test compared to control: $t(10) = 4.19$, $t(5) = 2.36$, $t(6) = 3.35$ for DA, SKF and Quin, respectively; $P = 0.002$, $P = 0.06$ and $P = 0.02$, respectively. Mean ± s.e.m. (red). (**d**) Mean ± s.e.m. (red) data show outward DA (30 μM) current before, during and after D2 receptor antagonist sulpiride (10 μM) treatment ($n = 6$ cells from 2 mice). One-way

repeated-measures ANOVA, $F(5,10) = 12.53$, $P = 0.0005$. Sulpiride versus control, $^{*}P = 0.014$, Bonferroni *post hoc* comparison. Holding potential −60 mV. (**e**) GFP-expressing ARC POMC neurons are contacted by red TH immunoreactive axons. Arrows point to TH-positive boutons in apparent contact with POMC neurons. Scale bar, 8 μm; typical of 3 mice. (**f**) DA (top, 30 μM) and SKF38393 (middle, 10 μM), but not quinpirole (bottom, 10 μM) excite NPY/AgRP neurons. (**g**) Depolarization of NPY/AgRP neuron membrane potential (mean ± s.e.m.) by DA ($n = 25$ cells from 9 mice), SKF38393 ($n = 10$ cells from 3 mice) and quinpirole ($n = 8$ cells from 3 mice). (**h**) Control and treatment firing rates of NPY/AgRP neurons in DA ($n = 22$ cells from 9 mice), SKF38393 ($n = 10$ cells from 3 mice) and quinpirole ($n = 8$ cells from 3 mice). DA versus Ctrl: $t(21) = 4.75$, $^{***}P = 0.0001$; SKF versus Ctrl: $t(9) = 5.136$, $^{***}P = 0.0006$; quinpirole versus Ctrl: $t(7) = 0.76$, $P = 0.47$, paired two-tailed t test. Mean ± s.e.m. (red).

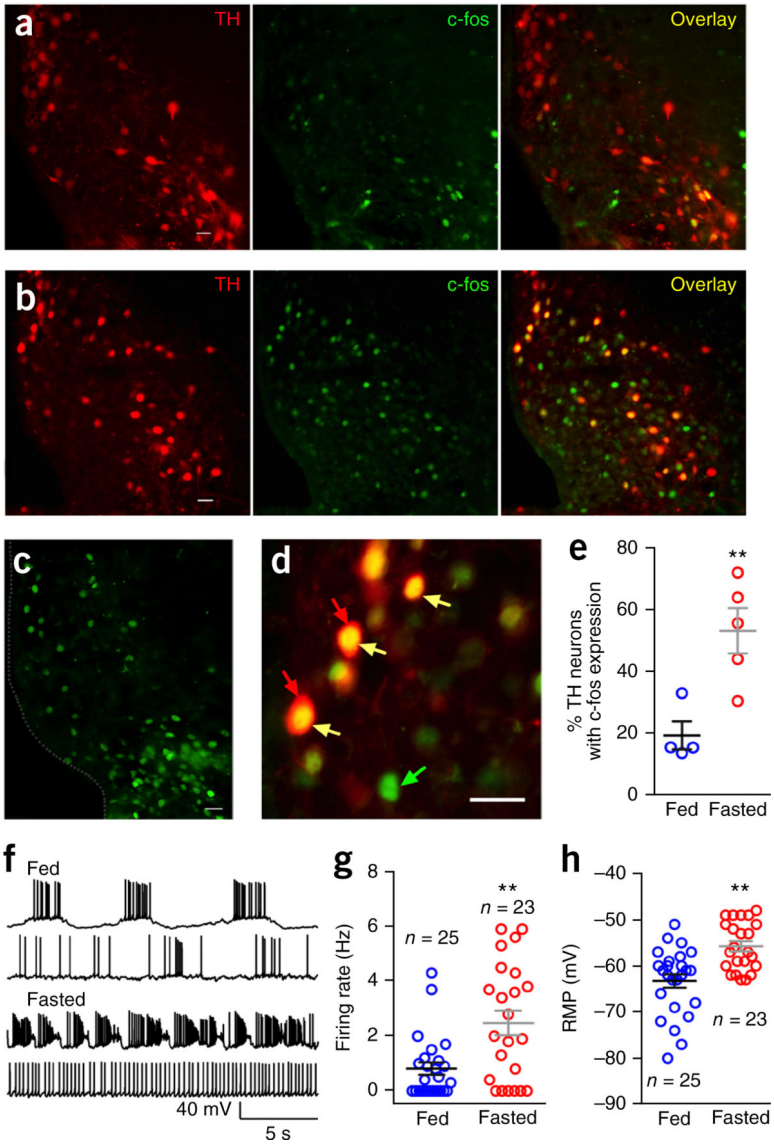

Figure 6.

Fasting increases c-fos expression and electrical activity in TH neurons. (**a**) Red fluorescence (left) shows ARC TH neurons from a normally fed control TH-tdTomato transgenic mouse. Scale, 20 μm. Green fluorescence (middle) shows c-fos immunoreactive ARC neurons from the same slice. Overlay image (right) shows coexpression of TH and c-fos from the normally fed mouse. (**b**) Red fluorescence (left) shows ARC TH neurons from a 24-h fasted TH-tdTomato transgenic mouse. Green fluorescence (middle) shows c-fos immunostained ARC neurons from the same slice. Overlay image (right) shows coexpression of TH and c-fos from the 24-h fasted mouse. Scale bar, 20 μm. (**c**) Another example showing c-fos immunoreactive ARC neurons in a slice from another mouse. Scale bar, 20 μm. (**d**) Higher magnification micrograph showing c-fos expressed in the nucleus of TH neurons. Scale bar, 20 μm. Red arrows point to TH-tdTomato cells, green arrow points to c-fos immunostaining in the nucleus and yellow arrows point to colocalization of TH and c-fos. (**e**) Percentage of TH neurons with c-fos expression from normally fed ($n = 4$) and 24-h

fasted mice ($n = 5$). Unpaired t-test, $t(7) = 3.673$. $^{**}P = 0.008$. Mean ± s.e.m. (**f**) Representative traces showing action potentials of TH neurons from normally fed and 24-h fasted mice. (**g**) Firing rates of TH neurons from 24-h fasted mice and normally fed control mice ($n = 25$ neurons from 6 fed mice and $n = 23$ neurons from 6 fasted mice). Unpaired t-test, $t(46) = 3.409$, $^{**}P = 0.0014$. Mean ± s.e.m. (**h**) Resting membrane potentials of TH neurons from normally fed ($n = 25$ cells from 6 mice) and 24-h fasted mice ($n = 23$ cells from 6 mice). Unpaired t-test, $t(46) = 4.075$, $^{**}P = 0.0002$. Mean ± s.e.m.

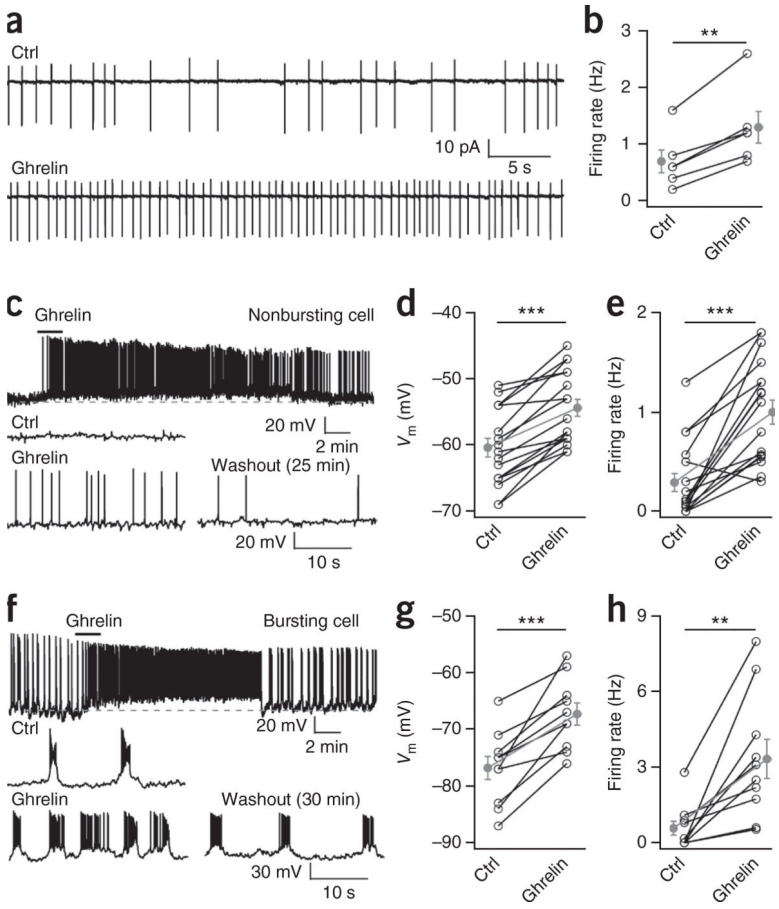

Figure 7.

Ghrelin excites arcuate TH neurons. (**a**) Traces show ghrelin (100 nM) increasing the spontaneous firing activity of a dorsomedial ARC TH neuron recorded in cell-attached configuration relative to baseline conditions (Ctrl). (**b**) Mean firing rate in control conditions and in ghrelin (n = 6 cells from 2 mice). Mean ± s.e.m. (gray). Ghrelin versus Ctrl: paired t test, $t(5) = 6.45$, $^{**}P = 0.001$. (**c**) Top, ghrelin produces long-lasting excitation in a nonbursting ARC TH neuron from whole-cell current-clamp recording. Bottom, expanded traces from the same neuron before, during and 25 min after ghrelin washout. (**d**) Mean membrane potential of nonbursting arcuate TH neurons in control conditions and in the presence of ghrelin (n = 17 cells from 9 mice). Mean ± s.e.m. (gray). Ghrelin versus Ctrl: paired t test, $t(16) = 8.13$, $^{***}P < 0.0001$. (**e**) Mean firing rate of a nonbursting TH neuron before and during ghrelin (n = 17 cells from 9 mice). Ghrelin versus Ctrl: paired t test, $t(16) = 6.46$, $^{***}P < 0.0001$. Mean ± s.e.m. (gray). (**f**) Top, ghrelin produces long-lasting excitation in a bursting arcuate TH neuron in whole-cell current-clamp recording. Bottom, expanded traces from the same neuron before, during and 30 min after ghrelin washout. (**g**) Mean membrane potential of bursting arcuate TH neurons at baseline (Ctrl) and in ghrelin (n = 10 from 6 mice). Mean ± s.e.m. (gray). Ghrelin versus Ctrl: paired t test, $t(9) = 6.015$, $^{***}P = 0.0002$. (**h**) Mean firing rate of bursting TH neurons before and in the presence of

ghrelin (n = 10 cells from 6 mice). Mean ± s.e.m. (gray). Ghrelin versus Ctrl: paired t test, $t(9) = 4.037$, $^{**}P = 0.003$.